Kufa Journal of Engineering
Vol. 7, No. 1, January, 2016, P.P.27-46
Received 13 July 2015, accepted 16 September 2015

THE EFFECT OF SOIL CAVITY ON LATERALLY LOADED SINGLE PILE BY USING THE FINITE ELEMENT METHOD

Nadher H. Al-Baghdadi[1]

[1] Asst. Lecturer / Faculty of Engineering /University of Kufa,
nadherlabaghdadi@gmail.com

ABSTRACT

The research presents a numerical study of the interaction between single cavity and adjacent pile in homogenous sandy soil by utilizing an efficient finite element formulation. A square cross sectional concrete pile, with (9) m length and (0.6) m width, has been used. The interface layer between pile and surrounding soil was represented by thin layer element.

The research results indicate that, in the direction perpendicular to the direction of applied load, where the ratio between the distance from the cavity to the pile and cavity length (measured in the same direction), is equal or more than (1.7) the effect of cavity can be neglected. While the values of the maximum bending moment decrease with increasing of the above mentioned ratio, and it became constant when the ratio ≥ (2.0). The deformations around cavity increases with increasing lateral load and decreasing the above mentioned ratio, particularly in the nearest side of pile and these deformations are constant when the ratio ≥ (2.0).

تأثير تجويف في التربة على ركيزة محملة بصورة افقية باستخدام طريقة العناصر المحددة

ناظر حسن جواد البغدادي

مدرس مساعد / قسم الهندسة المدنية/ كلية الهندسة / جامعة الكوفة

الخلاصة

يقدم البحث دراسة عددية حول العلاقة بين تجويف داخل تربة رملية متجانسة وركيزة متاخمة محملة بصورة افقية بأستخدام طريقة العناصر المحددة. تم استخدام ركيزة من الخرسانة ذات مقطع مربع بطول ظلع(0.6 م) وبطول(9 م). تم تمثيل التربة المحيطة بالركيزة بواسطة العنصر البيني ذو الطبقة الرقيقة.

تشير النتائج على انه يمكن اهمال تأثير الفجوة في حال كون نسبة المسافة بين الركيزة والفجوة (في الاتجاه العمودي على تسليط الحمل) الى طول الركيزة (في نفس الاتجاه العمودي لتسليط الحمل) عندما تكون اكبر او يساوي (1.7)، بينما تقل قيمة عزم الانحناء الاقصى بزيادة النسبة المذكورة اعلاه، ويصبح العزم الاقصى ثابتا عندما تكون النسبة المذكورة اعلاه ≤ (2.0). أن التشوه حول الفجوة يزداد بزيادة النسبة اعلاه وبالخصوص على الجانب الاقرب الى الركيزة ، ويصبح التشوه ثابتا عندما تكون النسبة المذكورة اعلاه ≤ (2.0).

1. INTRODUCTION:

The existence of cavities causes both vertical and lateral ground movements. For existing structures, the ground movement induced by cavities and activities such as tunneling may cause a reduction in bearing capacity of foundations as well as the development of additional settlement and lateral movements. Numerical simulations were conducted using finite element technique, to solve three dimensional problems of variations in the cavity location in Y-direction as seen in Fig. 1.

Review of literature indicates that there is few published information on the behavior of the pile foundation subjected to lateral loading for soils with the presence of cavities, Ziyazov (1976), examined the effect of trench on lateral pile by experiment work. Al-Mosawe et al. (2007), performed laboratory experimental models of laterally loaded piles in loose sandy soil, two cavities have been studied. Kadhim (2011) performed finite element model to examine the impact of cavity in clayey soil adjacent to axially loaded pile. Shlash et al. (2012) performed an experimental study of interaction between cavity and adjacent laterally loaded pile in sandy soil, batter pile was included in the study.

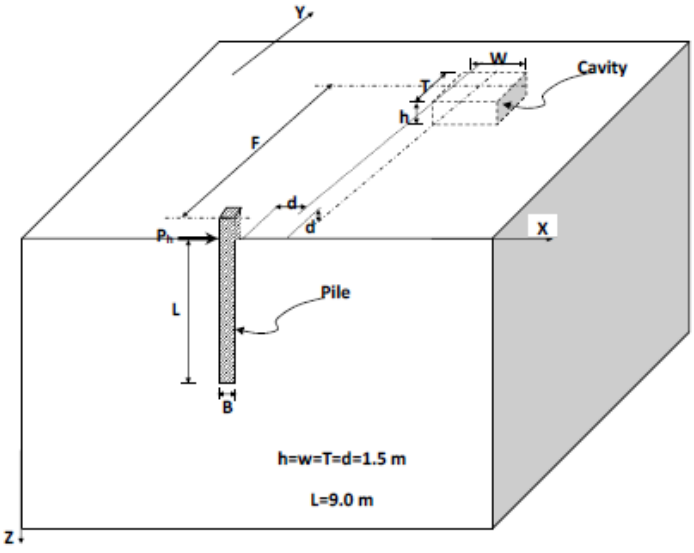

Fig. 1. Schematic diagram of the proposed model

2. FINITE ELEMENT PROGRAM:

A computer program was prepared by author by using FORTRAN 90 programming language to solve equilibrium equations of the finite element modeling, which is used in this study to analyze single pile embedded in sandy soil with cavity presence subjected to lateral load. Pile-load tests models were conducted using LCM (load control method). 20 nodes quadrilateral element was used. Elasto-Plastic model that do not incorporate time-dependent creep deformations have been generally adequate to predict long term field behavior. For the purpose of analysis, it was used that the, pile materials (concrete or steel) are assumed to be linearly elastic defined by the elastic modulus of elasticity and Poisson's ratio, while soil and interface materials behavior were assumed to be governed by nonlinear Elasto-Plastic constitutive model based on the Mohr-Coloumb failure criterion. Thin layer interface element, (Desai et al. 1984), has been used to represent the contact zone between pile and soil.

2.1. Validation of the Finite Element Program:

The verification of the program has been performed depending on the summarizing information from the literature review two field loading tests (Trochanis et al. (1991), Elrafei, (2003)),

Tables 1–4 show the properties of piles and soils for the models mentioned above. The comparisons between the results of the finite element program and two field loading tests explain good agreement as shown in Fig. 2 and 3. Depending upon these comparisons, the proposed finite element program in this research work appears to be capable of predicting lateral response of single pile with or without cavity presence with accuracy.

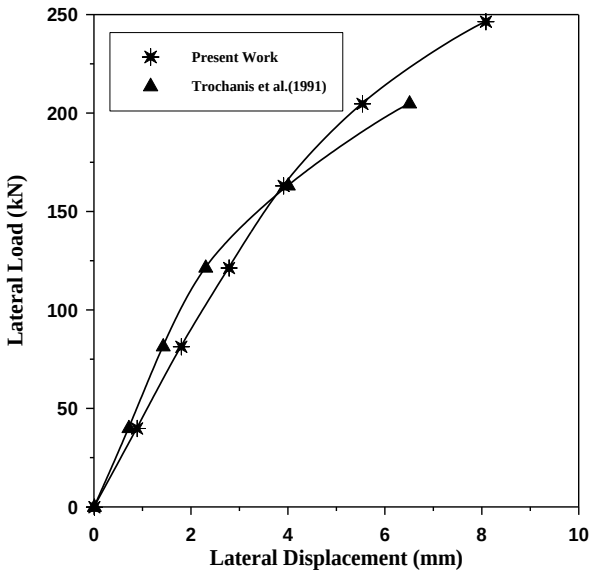

Fig. 2. Comparison between present study and Trochains et al. (1991) for square pile model

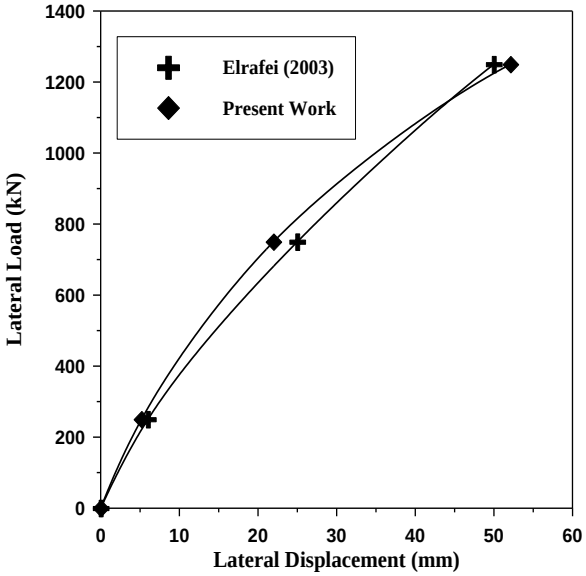

Fig. 3. Comparison between present study and Elrafei (2003) for rectangular barrette model

2.2. The Finite Element Model:

The results comprise the study of the variations of the cubical cavity locations in Y-direction (the cavity traction in the direction perpendicular to the paper) as seen in Fig. 3. The finite element mesh is not based on symmetry (full model is meshed) because of variation of cavity location in Y-direction. In the second category, due to symmetry only one half of the model is meshed. Twenty node brick elements are used for the soil, pile and interface. The soil domain considered from the center line of pile is (10 times) the cavity diameter in X and Y directions. The depth of soil considered below the pile tip is 0.8 times the length of the pile as seen in Fig. 3. The mesh is very fine in the upper part of the model to provide different shapes of the cavity. The element size gradually increases toward the boundaries of the model in all three dimensions. The range of the cross-section diameter of the cavities are from (0.5 m) to (1.5 m), therefore the cavity diameter used in this analysis is (d=1.5 m). The cavity idealized as a cubic shape with dimensions (1.5*1.5*1.5) m. For all model tests in this research work, the cavity position in X-direction and Z-direction are constant. In X-direction, the cavity is located at horizontal distance equal to cavity diameter (d=1.5 m) from the front face of the pile to the left side of the cavity, this distance is the same, in Z-direction but as a vertical distance from ground surface level to the cavity top as illustrated in Fig. 3.

Table 1. Concrete pile parameters (after Trochanis et. al., 1991)

Properties	Values
Width (B), m	0.5
Length (L), m	10
Modulus of elasticity(E_p),kN/m^2	20 000 000
Poisson ratio (ν)	0.3
Unit weight (γ), kN/m^3	23

Table 2. Soil parameters (after Trochanis et. al., 1991)

Properties	Values
Modulus of elasticity(E_s),kN/m^2	20 000
Poisson ratio (ν)	0.48
Undrained shear strength (Su), kN/m^2	20
Submerged unit weight (γ'), kN/m^3	11.8
Angle of internal friction (ϕ),deg.	0
Angle of dilation (ψ),deg.	0
Angle of friction (δ_a) ,deg.	0
Adhesion, (C_a) , kN/m^2	20

Table 3. Concrete barrette parameters (after Elrafei, (2003))

Properties	Values
Thickness (t), m	0.6
width (B), m	2.8
depth (L), m	14
Modulus of elasticity (E_p), kN/m^2	25 000 000
Poisson ratio (ν)	0.2
Unit weight (γ), kN/m^3	25

Table 4. Soil parameters (after Elrafei, (2003))

Properties	Values
Modulus of Elasticity (E_s), kN/m^2	15000
Poisson Ratio (ν)	0.3
Undrained Shear Strength (Su), kN/m^2	0
Unit Weight (γ), kN/m^3	16
Angle of internal friction (ϕ), deg.	29
Angle of dilation (ψ), deg.	0
Angle of friction (δ_a), deg.	21.75
Adhesion, (C_a), kN/m^2	0

Concrete piles were used in this analysis. The length, width, unit weight, modulus of elasticity and Poisson's ratio of this pile were chosen to be (9.0 m), (0.6 m), (24 kN/m^3), (200*10^5 kN/m^2) and (0.25) respectively.

The following parameters were used for sandy soil: friction angle (φ) of 38.5^0, modulus of elasticity (E) of 20125 kN/m^2, Poisson's ratio (υ) of 0.3, unit weight (γ) of 19.4 kN/m^3, Cohesion (c) of 21 kN/m^2, dilation angle (ψ) of 0^o.

The interface layer between pile and surrounding soil is represented by thin layer of elements (0.01 to 0.1 from the width of the element, Desai et al., (1984). All interface elements were simulated by Mohr-Coulomb model with a friction angle ($\delta_a=33^0$) Potyondy (1961).

The analysis were conducted by using load control at pile head (e/L=0). The ultimate lateral capacity of the pile is taken as the load corresponding to a deflection equal to (0.2) times the diameter of the pile on the load-deflection curves (Broms, 1964).

The parameters of the proposed model are shown in Fig. 3. These parameters are defined as follows:

(F) is the distance between the centerline of the pile and the centerline of the cavity in Y-direction.

(T) is depth of the cavity.

(h) is height of the cavity.

(w) is width of the cavity.

(B) is width of the pile

(L) is length of the pile.

(P_h) is lateral load increments

(d) is the vertical distance from the ground surface level to the cavity top or the horizontal distance from the pile facing to the left side of the cavity.

The bending moment (M) in pile was computed by the program based on the following equation:

$$M = -EI.\frac{d^2y}{dx^2} = -\frac{EI}{r^2}(y_1 - 2y_o + y_3) \quad (1)$$

Where E: modulus of elasticity of the pile.

r: vertical distance between any two points

I: moment of inertia of the pile.

$\frac{d^2y}{dx^2}$: Curvature of the pile obtained by numerical differentiation of slope measured by program.

3. RESULTS AND DISCUSSION.

3.1. Influence of Cavity Position in Y-Direction:

Lateral load – horizontal displacement curves (P-Y curves) were generated for the cavity cases with (F/T=0, 0.2, 0.3, 0.7, 0.8, 1.0, 1.3, 1.7, 2.0 and 3.0), in additional to no cavity case as shown in Fig. 4. The horizontal loading procedure started with increments of (100 kN) and a maximum final load of (1200 kN). The value of the final load is greater than the load corresponding to deflection of (20 %) of the pile diameter (i.e ultimate lateral load=900 kN). This load of (900 kN) is found from the load – displacement curve of the intermediate case between no cavity and (F/T=0) conditions. It is interesting to note that the load-displacement curve for no cavity condition exhibits strong hardening, also the curve of this case is similar to the curves of cavity cases at positions (F/T= 1.7, 2.0 and 3.0) in values (the cavity effects are

eliminated at distance F/T≥1.7). This is due to the fact that the cavity with (F/T≥1.7) does not exist in the region of the passive stability of the pile (at the pile facing). It should also be noted that the load-displacement curves for all the eleven models are the same up to (400 N) load, beyond this load the cavity models with (F/T≥1.7) carries more load than the models with (F/T<1.7). Also, the Fig. 4 illustrates the effects of the cavity position in Y-direction are very high for the cases (F/T=0 and 0.2) and generally decrease with increasing of the distance between the cavity and pile (F/T). Also, from this figure, the load-displacement curves of model tests with (F/T=0 and 0.2) are very much closer to each other at any value of lateral load increments. This (P-Y) approach has been widely used to design piles subjected to lateral loading.

For ultimate lateral thrust of (900 kN), the effect of varying (F/T) on the relation between horizontal displacement with depth is shown in Fig. 5. It is noted that the displacement-depth curves of the cases (F/T=1.3, 1.7, 2.0 and 3.0) test are very much closer with the model of the no cavity condition. In other means, at high lateral load (900 kN), the influence of the cavity on the lateral displacement at any depth is ignored when the cavity is located at position (F/T≥ 1.3). Similar results of the lateral displacements with depth were noted for the cases with (F/T= 0 and 0.2) and these results of the two cases are larger than those for other cases (F/T=0.3, 0.7, 0.8, 1.0, 1.3, 1.7, 2.0 and 3.0).

Fig. 6 depicts the variation of the lateral displacement with depth at ratios (F/T) from (0) to (3.0). Fig. 6-a followed the same trend as in the other cases. It is clear that the maximum values of the lateral displacements are observed at the ground surface level, then these values decrease with the increase of the depths below ground surface level as well as the change of sign for the lateral displacement is moving only between the depths (-6.0 m for the cases no cavity and cavity with F/T≥1.7) to (-6.5 m for the cases when the cavity at regions F/T<1.7) for any load increments. In other words, the point of the sign change is the center of the pile rotation. Also, Fig. 6 presents a comparison among the curves of the displacement- depth for magnitudes of lateral load from 100 N to 1200 N. The analysis of this figure shows that as load increases, the discrepancy between the curves increases.

Fig. 7 shows the distribution of the bending moment along the pile length due to an applied lateral loads on an unrestrained pile head, plotted for the case of soil without cavity and the cases with (F/T=0, 0.2, 0.3, 0.7, 0.8, 1.0, 1.3, 1.7, 2.0 and 3.0).

Moreover, the bending moment diagrams for all cases are similar in behavior except the case of the cavity with (F/T=0.2), Fig. 7-b. At shallow depth the magnitudes of the moment steadily increase with depth, till it reaches to positive maximum value at depth of (-2.625 m). Beyond these values steady decreases in moments at any lateral load increments and for the cases (F/T=0, 0.3, 0.7, 0.8, 1.0, 1.3, 1.7, 2.0 and 3.0), in additional to no cavity condition. In other words, for these cases the point of the maximum bending moment is independent of the cavity position in Y-direction.

For the case of cavity position with (F/T=0.2) and at any lateral load, the magnitudes of the maximum bending moment are of negative sign. The negative maximum moment is located at depth (-1.875 m) below the ground level. This is due to the fact that the cavity position leads soil particles toward the left side of the cavity only and hence the pile bends and twists.

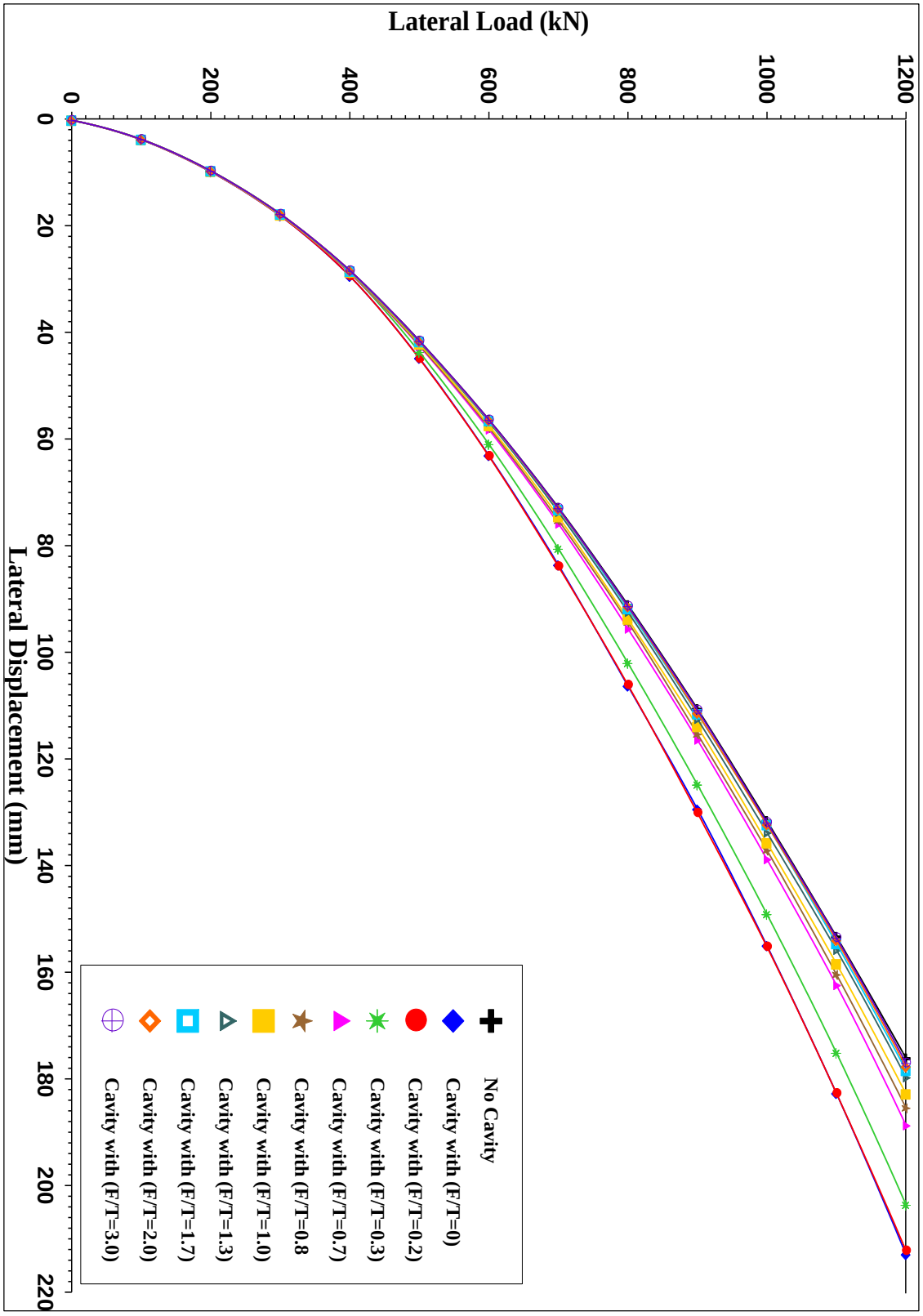

Fig. 4. Influence of cavity position in Y-direction (F/T) on lateral load-displacement curves

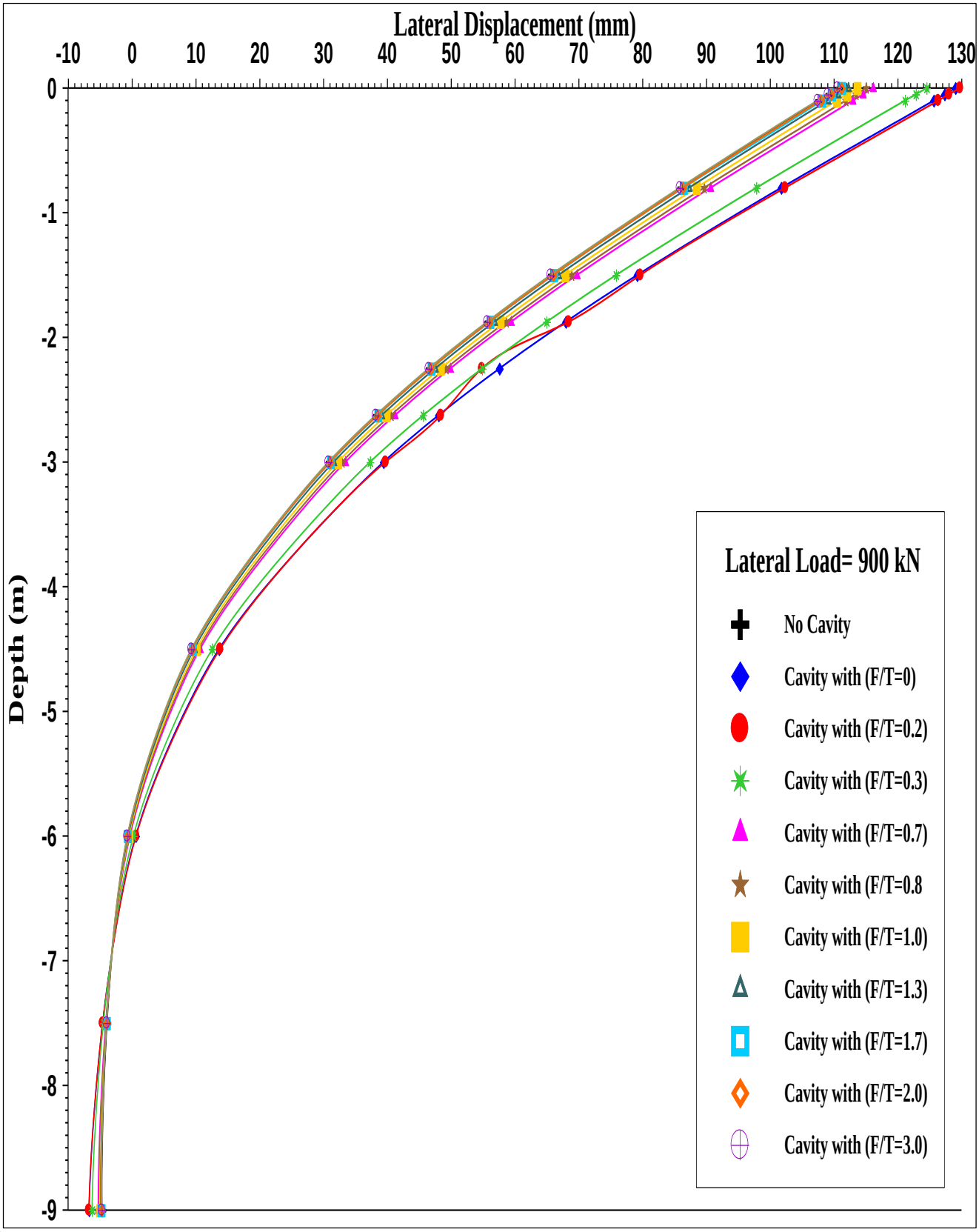

Fig. 5. Comparison among the lateral displacement distribution with depth for cavity positions (F/T=0, 0.2, 0.3, 0.7, 0.8, 1.0, 1.3, 1.7, 2.0 and 3.0) in additional to no cavity condition at lateral thrust of (900 kN)

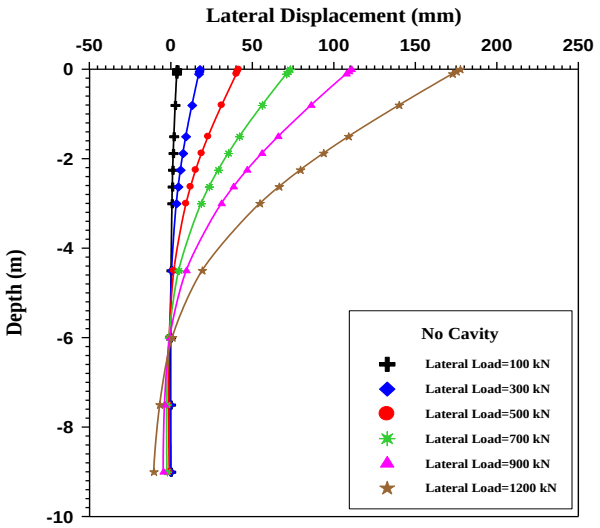

(a). horizontal displacement of pile facing versus depth for no cavity case

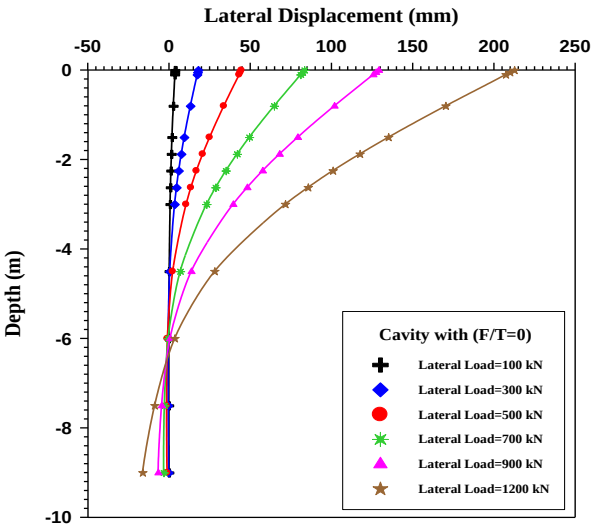

(b). Lateral displacement versus curves depth for case (F/T=0)

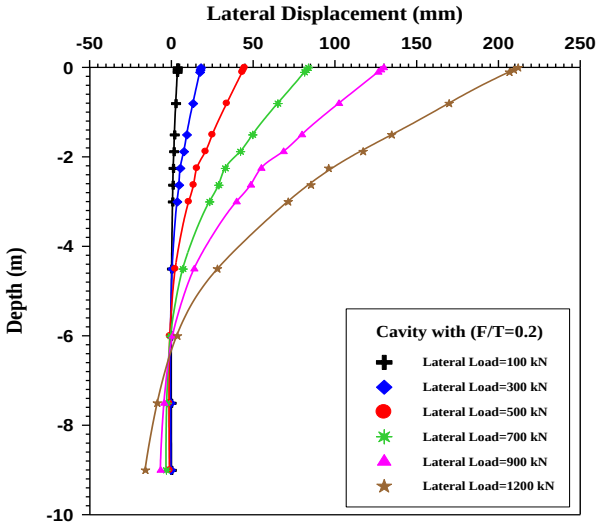

(c). Lateral displacement-depth curves for case (F/T=0.2)

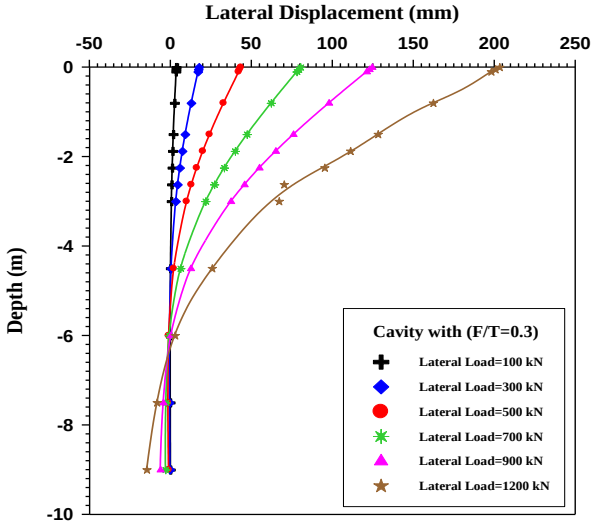

(d). Lateral displacement distribution curves with depth for case (F/T=0.3)

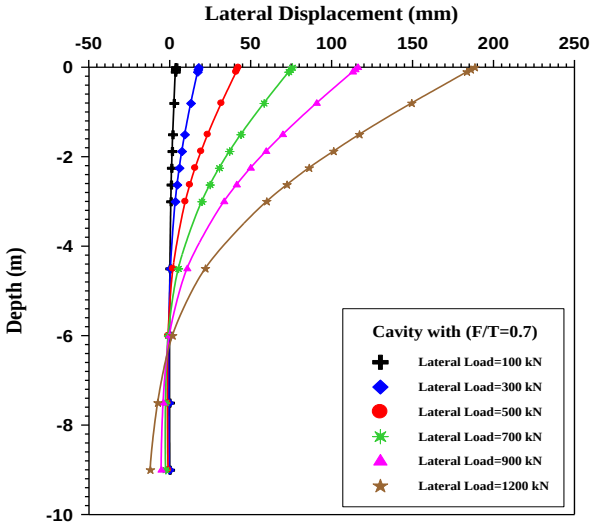

(e). Lateral displacement-depth curves for case (F/T=0.7)

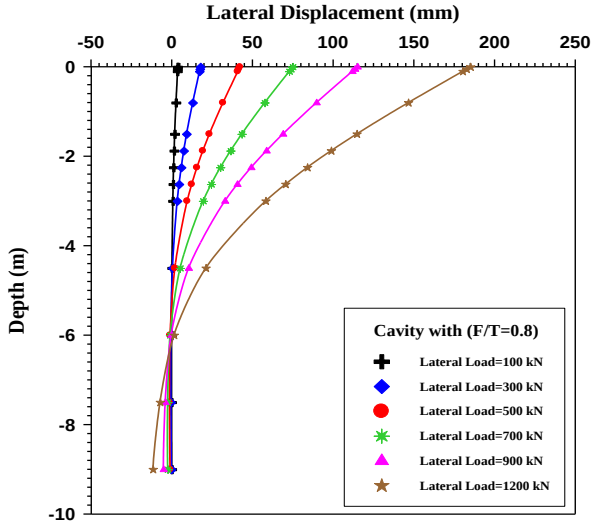

(f). Lateral displacement versus depth curves for case (F/T=0.8)

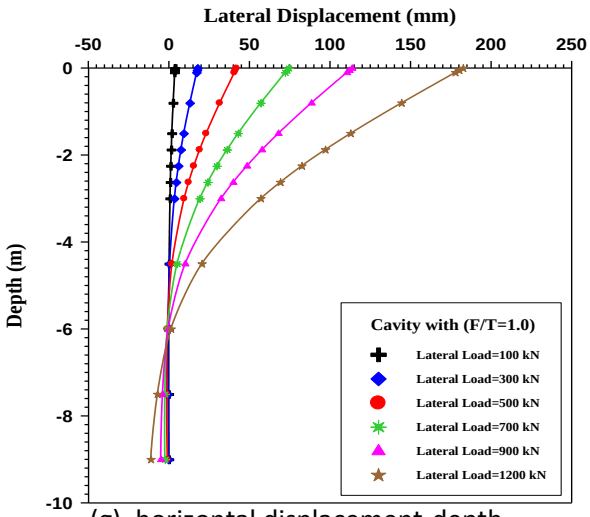

(g). horizontal displacement-depth curves for case(F/T=1.0)

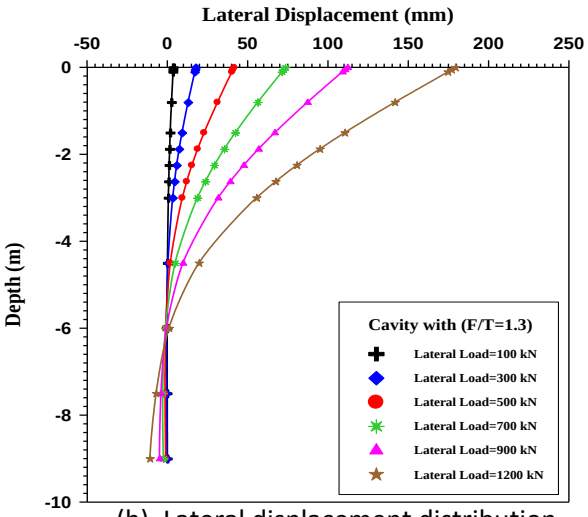

(h). Lateral displacement distribution curves with depth for case (F/T=1.3)

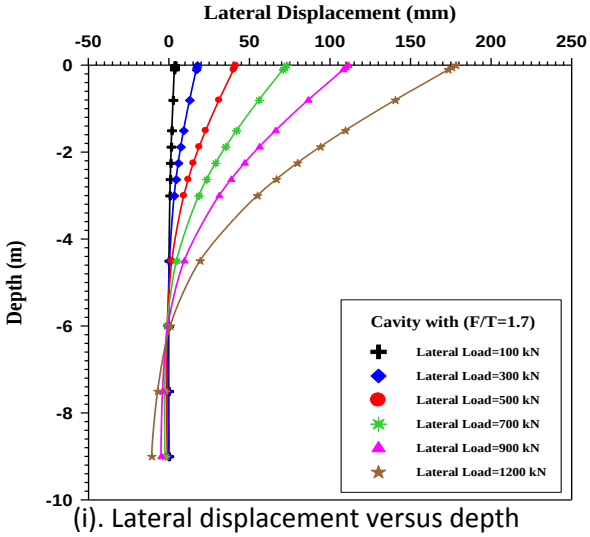

(i). Lateral displacement versus depth curves for case (F/T=1.7).

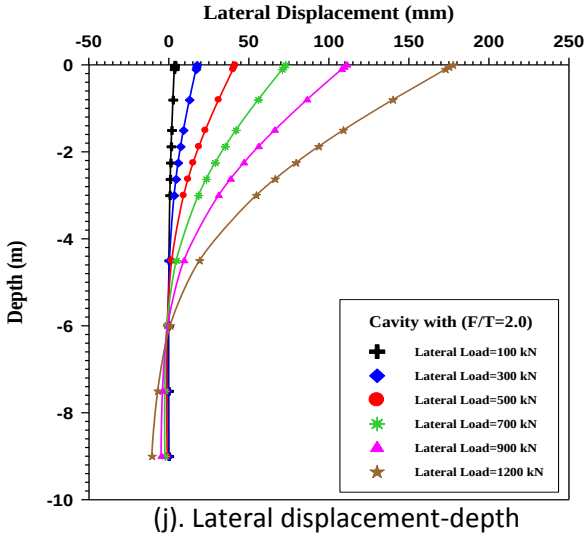

(j). Lateral displacement-depth curves for case (F/T=2.0)

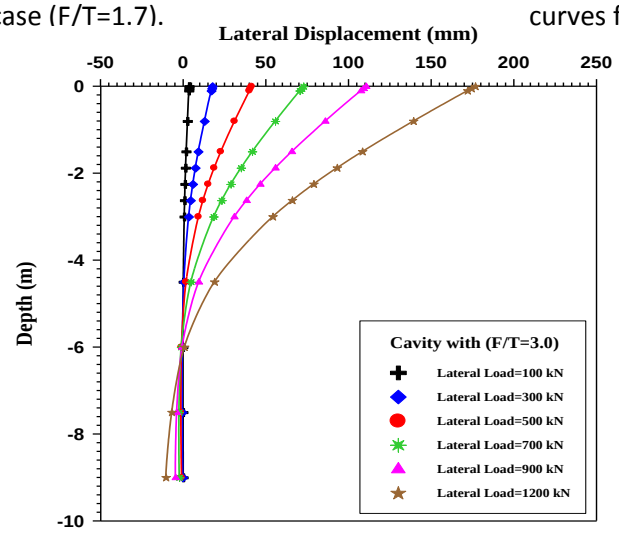

(k). Lateral displacement distribution curves with depth for case (F/T=3.0)

Fig. 6. Curves showing lateral displacement versus depth (below natural ground surface) at several lateral load levels

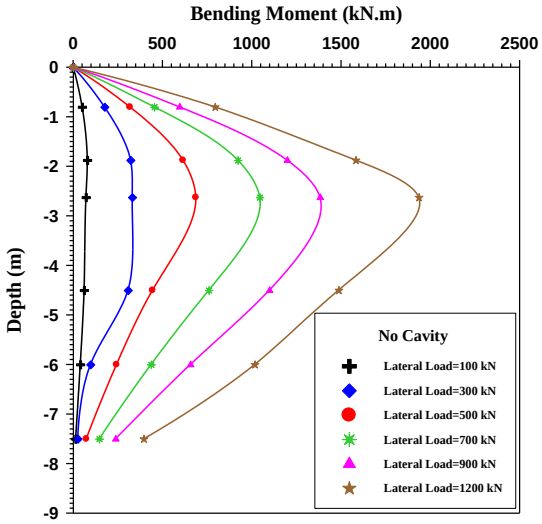

(a). Bending moment versus depth curves for no cavity case

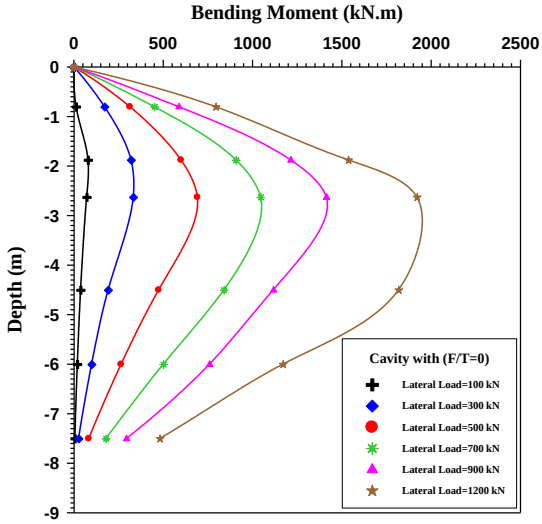

(b). Bending moment distribution curves with depth for case (F/T=0)

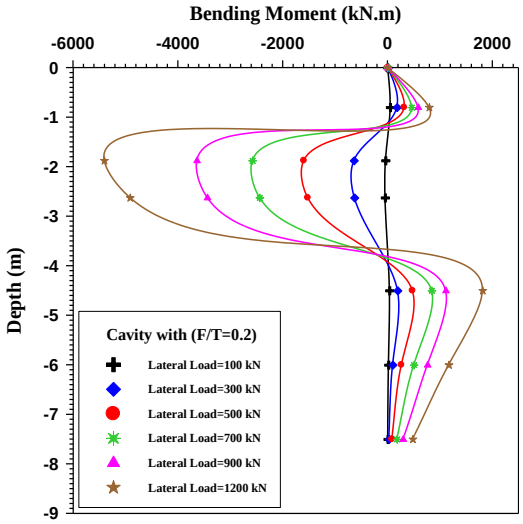

(c). Bending moment-depth curves for case (F/T=0.2)

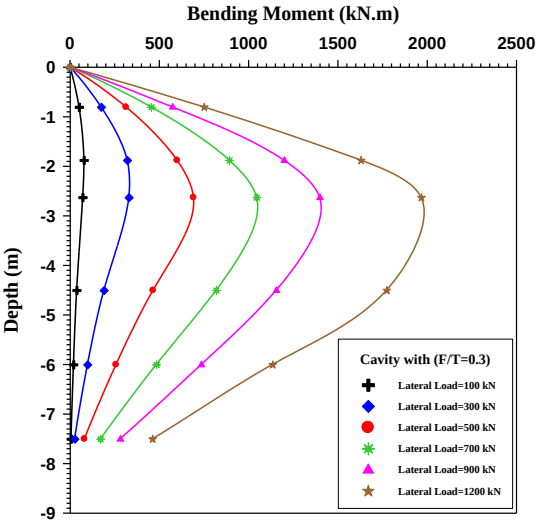

(d). Bending moment versus depth curves for case (F/T=0.3)

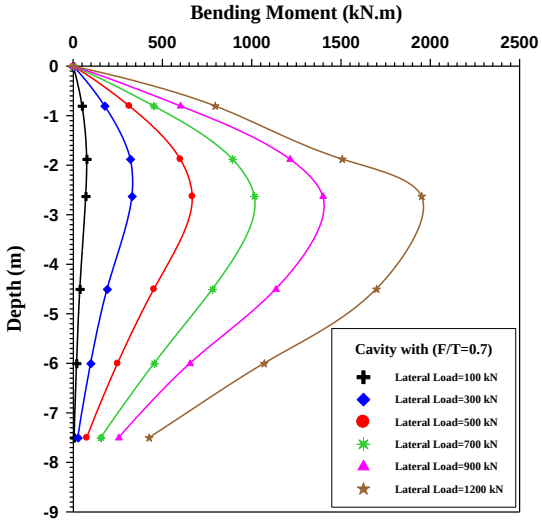

(e). Bending moment distribution curves with depth for case (F/T=0.7)

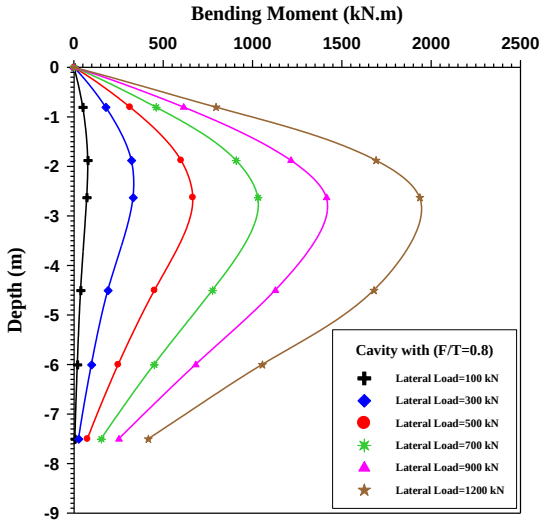

(f). Bending moment-depth curves for case (F/T=0.8)

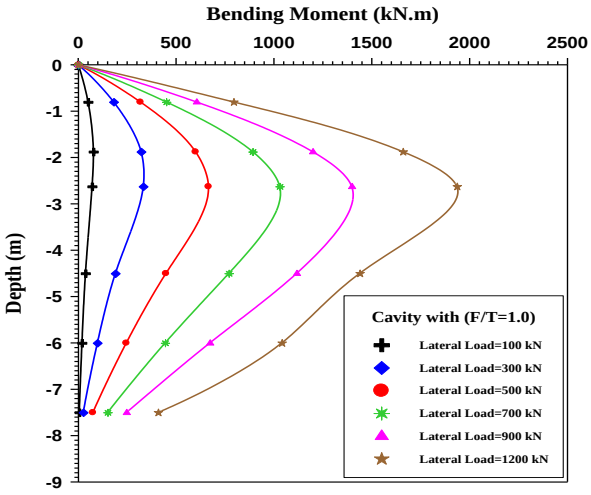

(g). Bending moment versus depth curves for case(F/T=1.0)

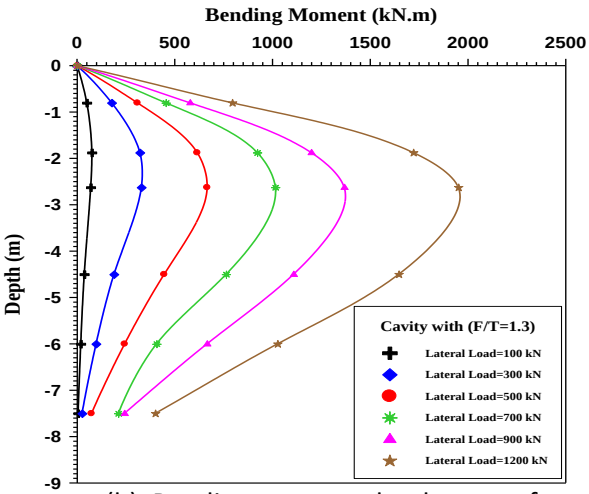

(h). Bending moment-depth curves for case (F/T=1.3)

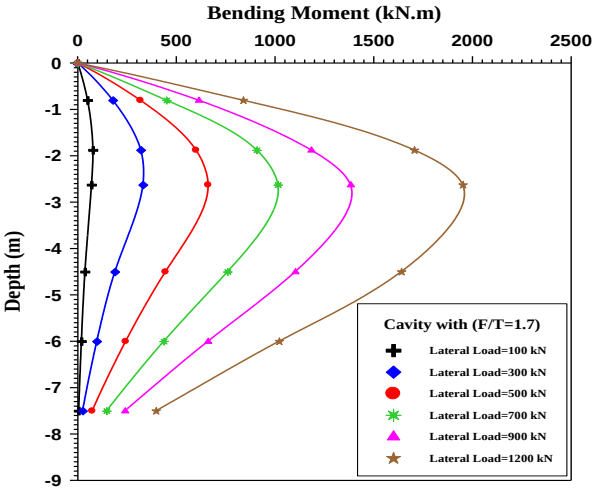

(i). Bending moment distribution curves with depth for case (F/T=1.7).

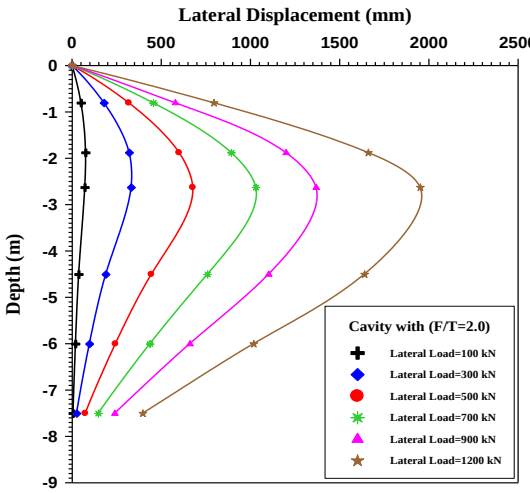

(j). Bending moment versus depth curves for case (F/T=2.0)

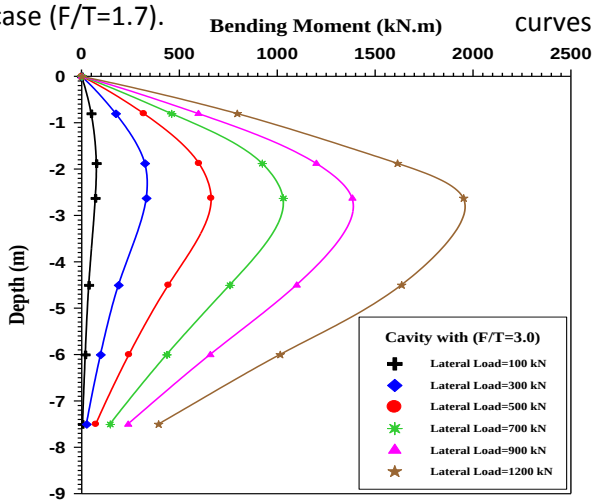

(k). Bending moment-depth curves for case (F/T=3.0)

Fig. 7. Bending moment distributions with depth at various lateral load level and at different cavity locations

Fig. 8 presents the influence of the cavity position in Y-direction (F/T) on the bending moment distribution along the pile due to lateral load of (900 kN) for all cases except the case of (F/T=0.2). It can be seen that equal values of the moment with shallow depths from ground surface level, the differences in magnitudes are started at maximum bending moment and it continued for greater depths. The magnitude of the maximum bending moment for a cavity position (F/T=0) is greater than that for the other cases. These maximum values of the bending moment are equal when the cavity is located at position (F/T≥2.0).

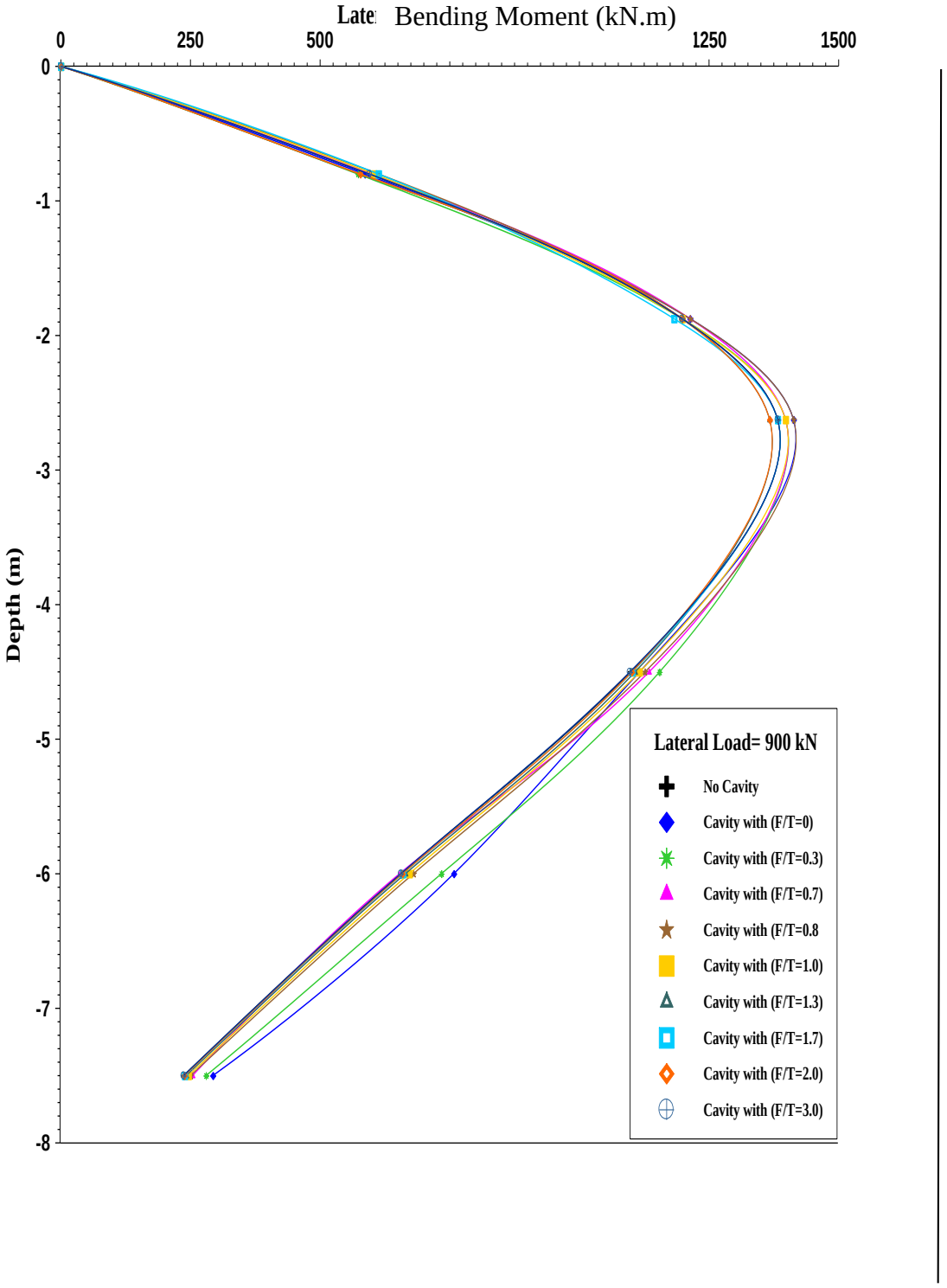

Fig. 8. Comparison among bending moments of pile for cases F/T=0,0.3,0.7,0.8,1.0,1.3,1.7,2.0 and 3.0) in additional to no cavity condition at lateral load equal to 900 kN

The distribution of the deformations due to lateral loading around the cavity center in Y-direction (the cross section of the cavity deformations at distance F/T) were calculated and can be seen in Figs. 9–18 for the cases of the cavity position (F/T=0, 0.2, 0.3, 0.7, 0.8, 1.0, 1.3, 1.7, 2.0 and 3.0) respectively. It can be seen from Figs. 9–18 that the higher generated deformations in the left side of the cavity are noted when the cavity is located at small ratios (F/T=0 and 0.2) for several values of the lateral load, this is because that the soil particles are moved laterally toward the left sides of the cavity when the cavity is existed in the influence zone of the pile. These deformations of the left side of the cavity diminish for the cases with (F/T= 0.3, 0.7, 0.8, 1.0, 1.3, 1.7, 2.0 and 3.0). In other words, the deformations around the cavity increase with increasing of the lateral load increments and with decreasing of the cavity position ratio (F/T).

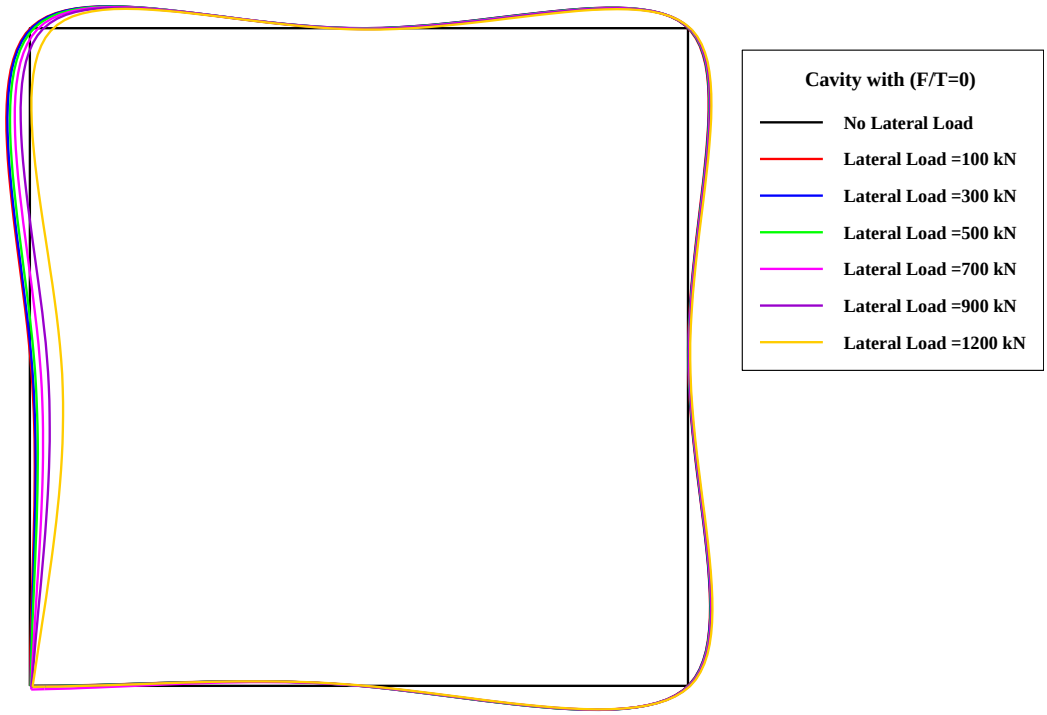

Fig. 9. Propagation of the deformation zones of the cavity for case (F/T=0) at several lateral loading

Fig. 10. The deformation of the cavity sides for case (F/T=0.2) at different lateral loading

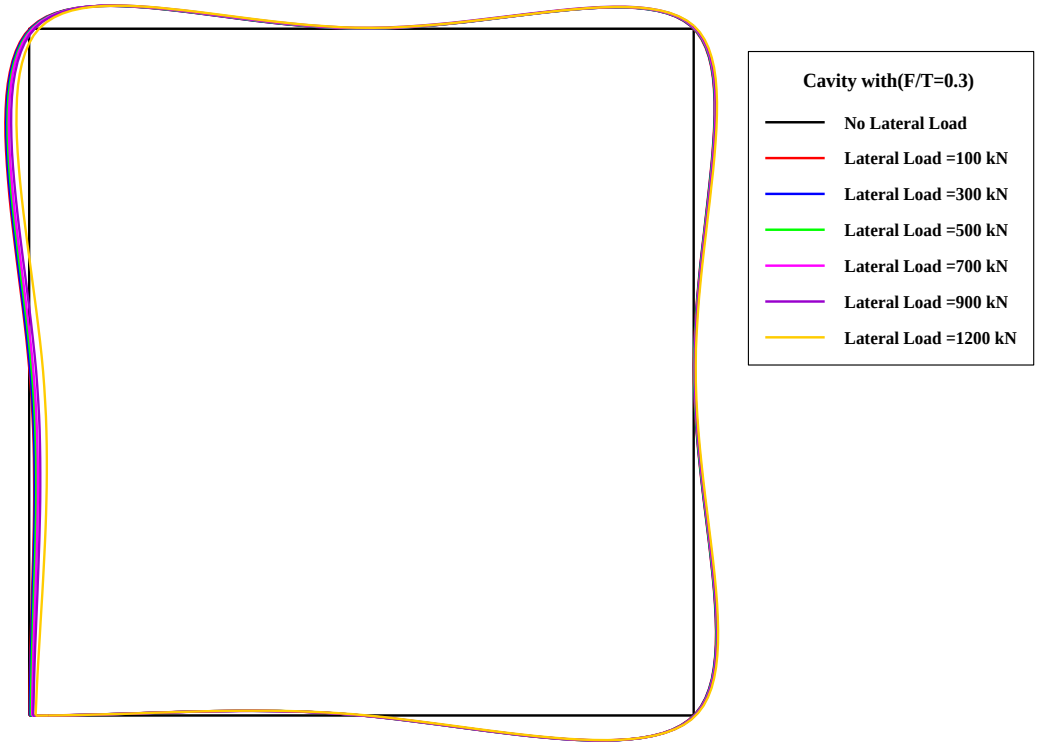

Fig. 11. Deformed shapes of the cavity for case (F/T=0.3) at different lateral loads

Fig. 12. The cavity deformations for case (F/T=0.7) at various lateral loads level

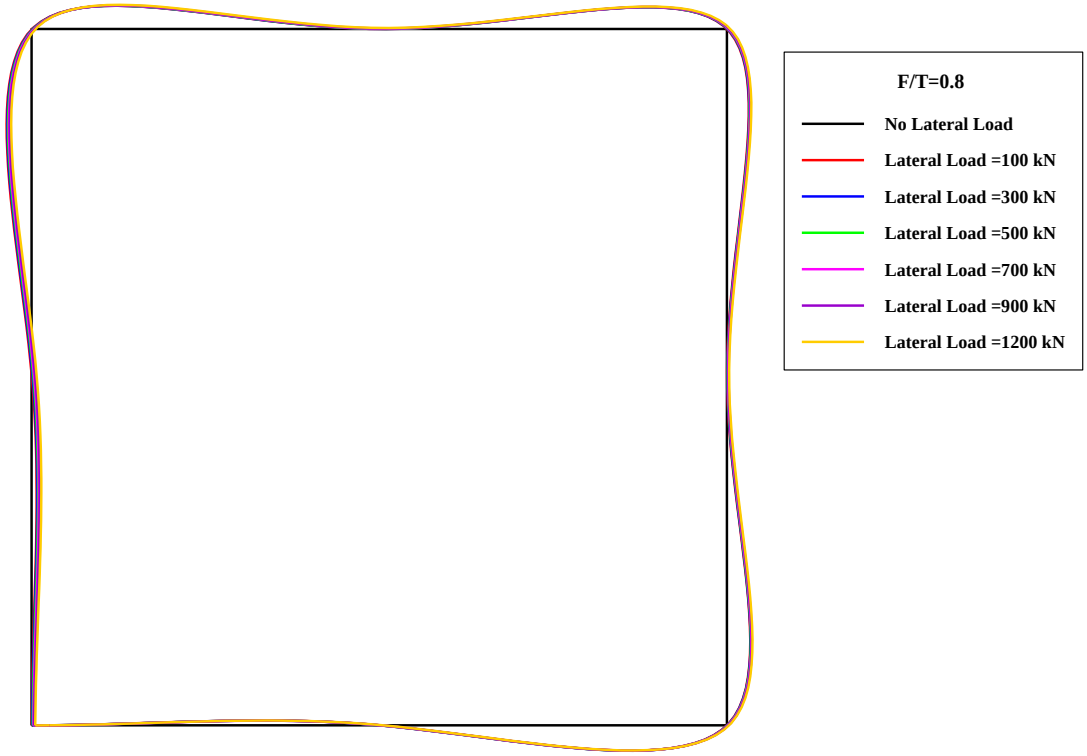

Fig. 13. Propagation of the deformations of the cavity side for case (F/T=0.8) at several lateral load level

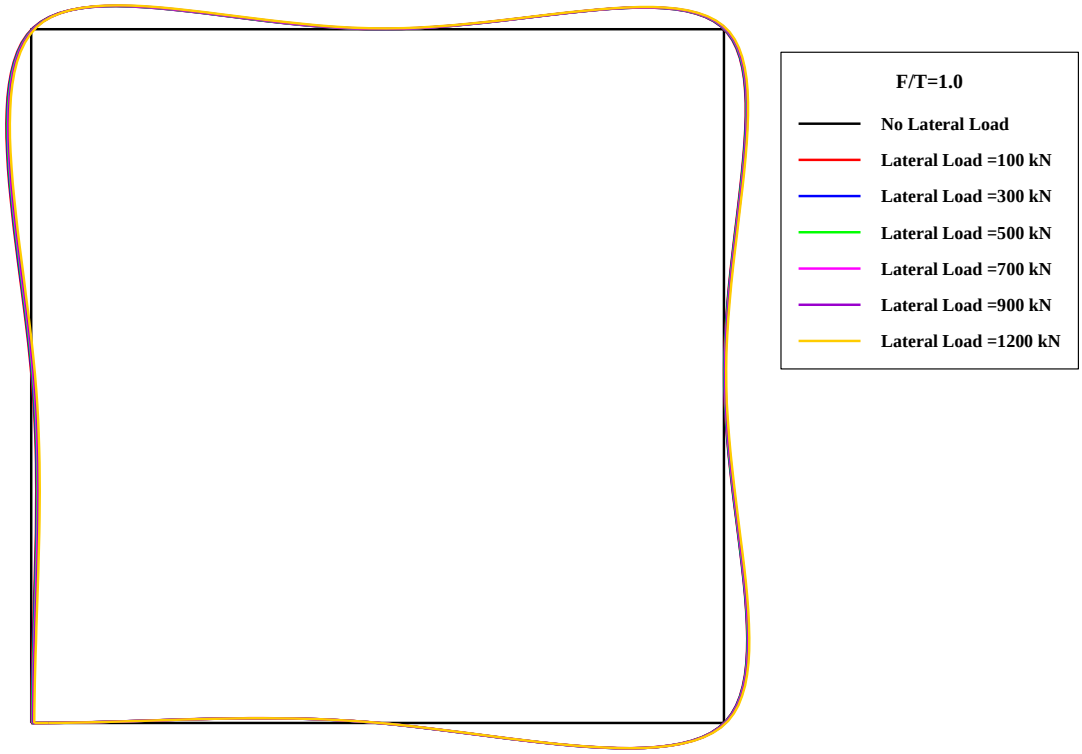

Fig. 14. The deformations of the cavity sides for case (F/T=1.0) at different lateral loading

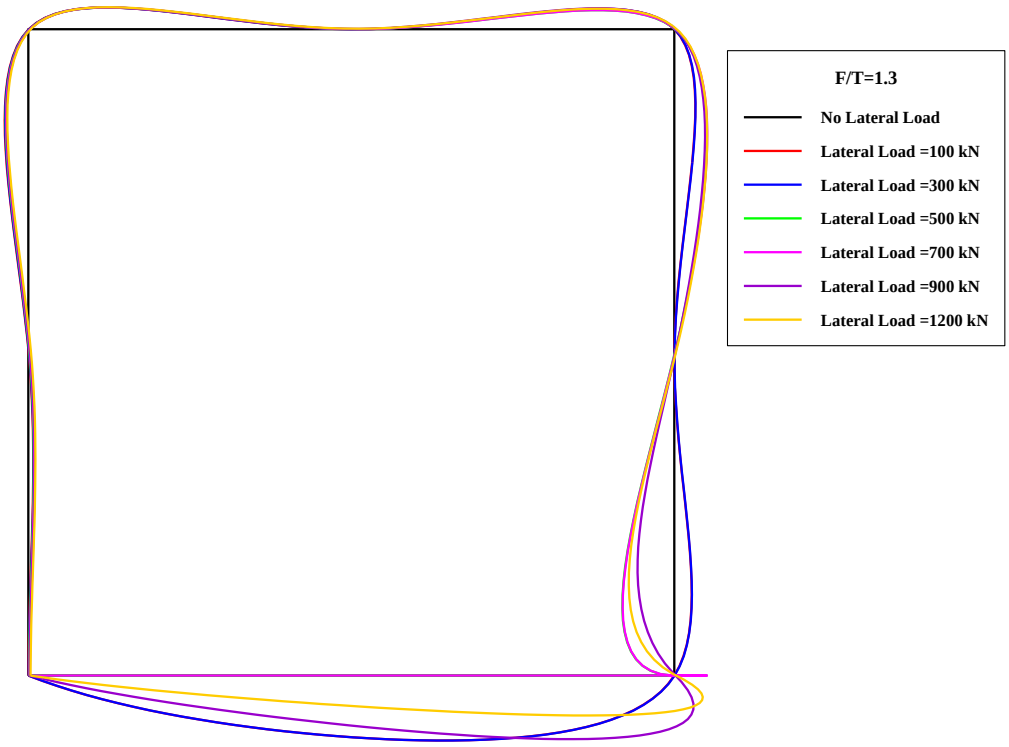

Fig. 15. The deformation zones of the cavity for case (F/T=1.3) at various lateral loading

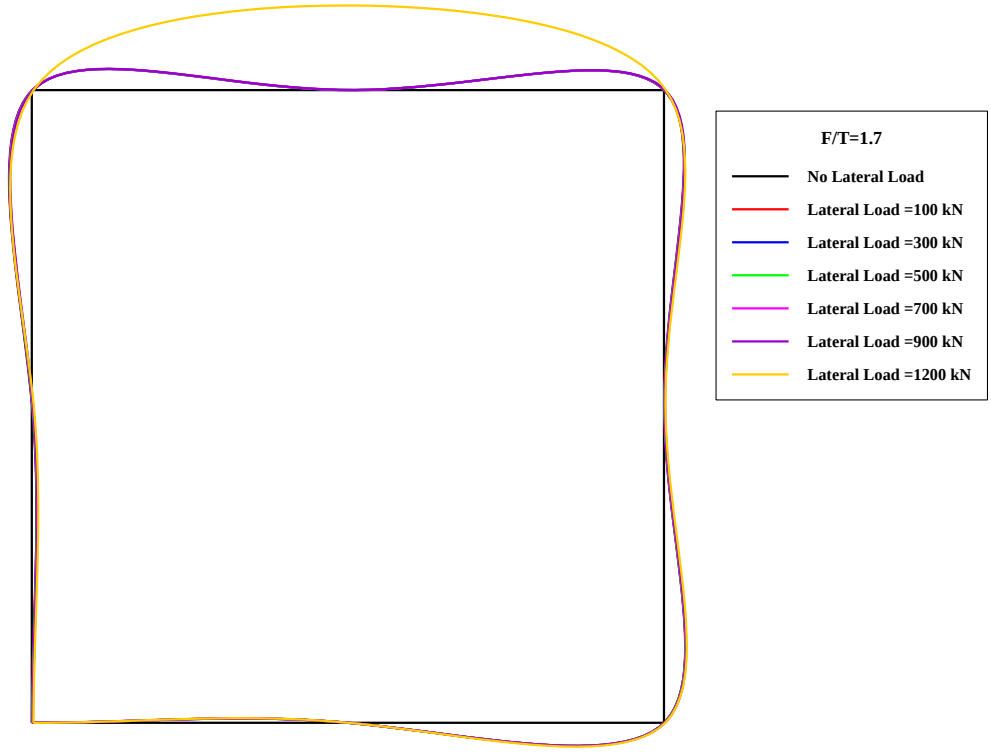

Fig. 16. The deformations of the cavity sides for case (F/T=1.7) at different lateral loading

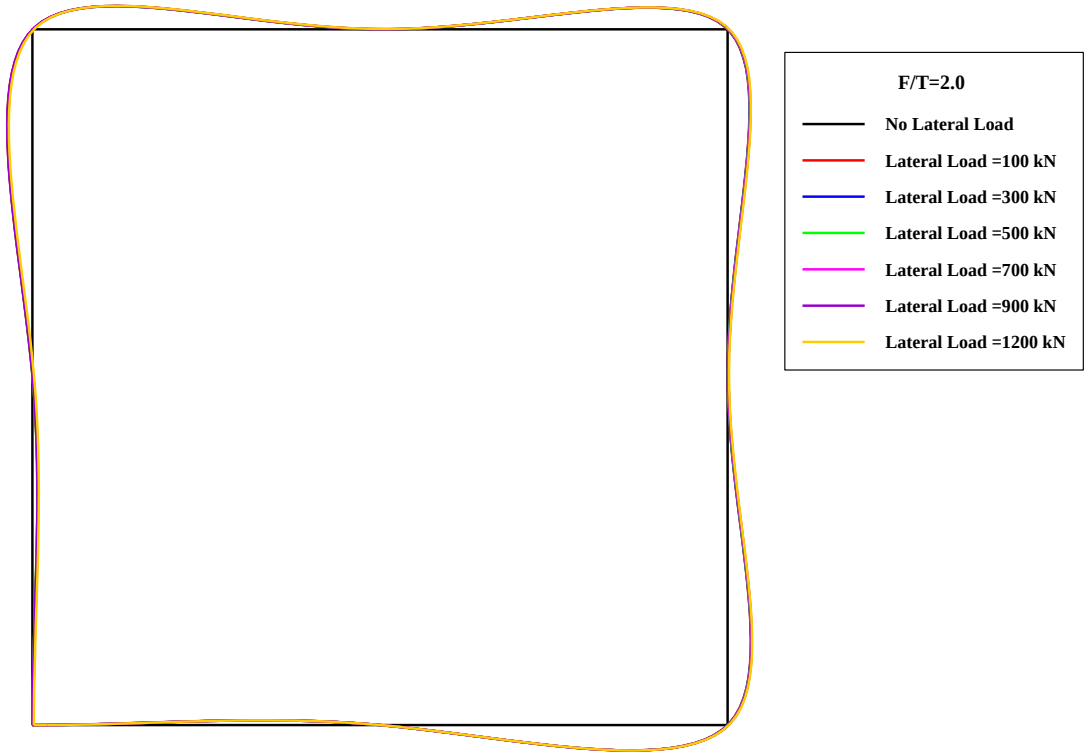

Fig. 17. Deformed shapes of cavity for case (F/T=2.0) at different lateral loads

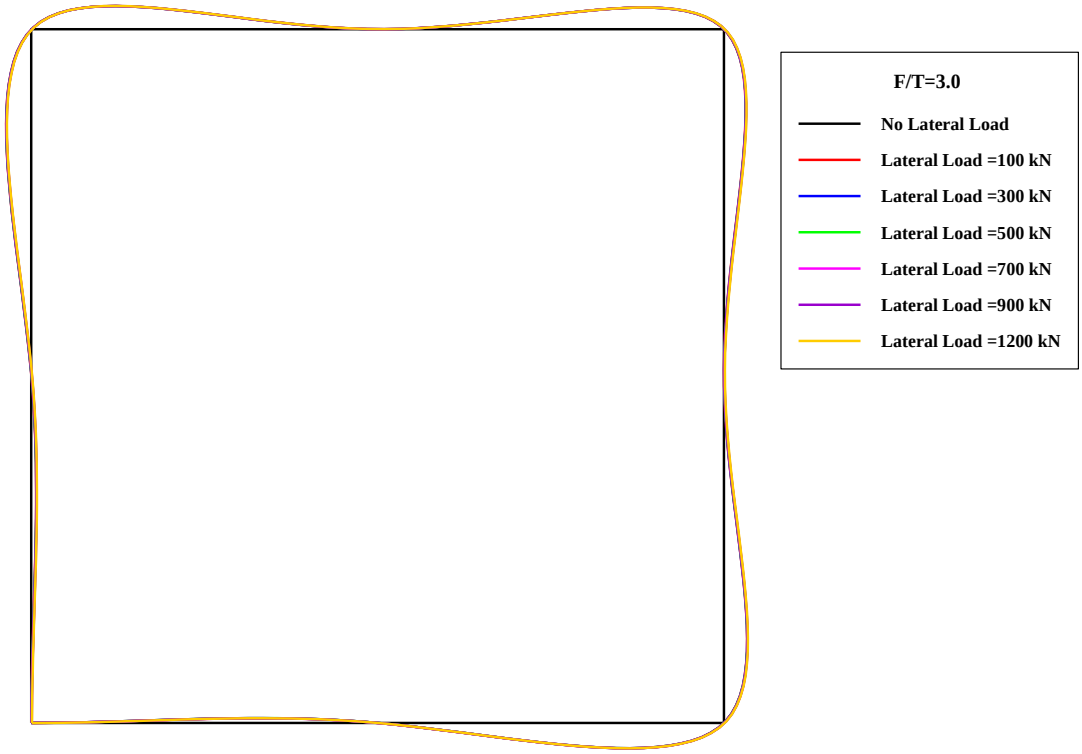

Fig. 18. The cavity deformations for case (F/T=3.0) at various lateral loading

4. CONCLUSIONS:

1. The influence of the cavity can be neglected when (F/T≥1.7).
2. Lateral displacements with load or with depth are equal for the two positions of the cavity (F/T=0 and 0.2), while the maximum bending moment of the cavity position (F/T=0) are positive value and changes to negative for cavity position (F/T=0.2). The centers of the pile rotation are located at depth (-6.0 m) below ground surface level for the cases with (F/T≥ 1.7) and increases to (-6.5 m) for other cases (F/T<1.7).
3. The value of the maximum bending moment decreases with increasing the distance between the cavity and pile (F/T). The magnitudes are constant when the ratio (F/T) becomes ≥2.0.
4. The deformations around cavity increases with increasing lateral load and decreasing (F/T), particularly in the left side of the cavity and these deformations are constant at cavity position (F/T≥2.0).

5. REFERENCES:

1. Al-Mosawe, M.J., Al-Shakarchi, Y.J., Al-Taie, S.M.," Embedded in Sandy Soils with Cavities", *Journal of Engineering*, Vol. 13, No.1, pp.1168-1187, (2007).
2. Broms, B.B., "Lateral Resistance of Piles in Cohesionless Soils", *Journal Soil Mechanics Division*, ASCE, Vol.90, No.3, PP.123-156, (1964).
3. Desai, C.S., Zaman M.M., Lightner, J.G., and Siriwardane, H.J.," Thin Layer Element for Interfaces and Joints", *International Journal of Numerical and Analytical Methods in Geomechanics*, Vol. 8, pp 19-43, (1984).

4. Elrafei, A.M., "Three-Dimensional Analysis of Laterally Loaded Barrettes in Sand", *Tenth International Colloquium on Structural and Geotechnical Engineering*, April,22-24,2003,Ain Shams University, Cairo, Egypt, (2003) .
5. Kadhim, Sh.T., " Studying the Behavior of Axially Loaded Single Pile in Clayey Soil with Cavities", *Eng. & Tech. Journal*, Vol. 29, No. 8, pp. 1619-1630, (2011).
6. Potyondy, J. G., "Skin Friction Between Various Soils and Construction Material," *Geotechnique*,Vol. 11, No. 4, pp.339–353, (1961).
7. Shlash, K.T., Mahmoud, M.R., Aziz, L.J.," Lateral Resistance of a Single Pile Embedded in Sand with Cavities", *Eng. & Tech. Journal*, Vol. 30, No. 15, pp. 2641-2663, (2012).
8. Trochanis, A. M., Bielak, J. and Christiano, P.," Simplified Model for Analysis of One or Two Pile", *Journal of Geotechnical Engineering Division*, ASCE, Vol.117, No.3, PP 448-465, (1991).
9. Ziyazov, Ya. Sh., "Performance characteristics of horizontally loaded piles located near a trench", Soil Mechanic and Foundation Engineering, ASCE. Vol. 13, No.3, p.p. 165-167, (1976).